General Disclaimer

One or more of the Following Statements may affect this Document

- This document has been reproduced from the best copy furnished by the organizational source. It is being released in the interest of making available as much information as possible.

- This document may contain data, which exceeds the sheet parameters. It was furnished in this condition by the organizational source and is the best copy available.

- This document may contain tone-on-tone or color graphs, charts and/or pictures, which have been reproduced in black and white.

- This document is paginated as submitted by the original source.

- Portions of this document are not fully legible due to the historical nature of some of the material. However, it is the best reproduction available from the original submission.

Produced by the NASA Center for Aerospace Information (CASI)

Space Shuttle Crawler Transporter Vibration Analysis
In Support of Rollout Fatigue Load Spectra Verification Program

Karl A. Meyer, Shaun M. Nerolich,
Roy C. Burton, Armand M. Gosselin
United Space Alliance, John F. Kennedy Space Center, Fl, USA
Ravi N. Margasahayam
NASA, John F. Kennedy Space Center, Fl, USA

Abstract

The Crawler Transporter (CT), designed and built for the Apollo Program in the 1960's and surpassing its initial operational life, has become an integral part of the Space Shuttle Program (SSP). The CT transports the Space Shuttle Vehicle (SSV) stack, atop the Mobile Launch Platform (MLP), from the Vehicle Assembly Building (VAB) to the launch pad. This support structure provides hydraulic jacking, leveling and load equalization for the 12 million pound stack on its 3.5-5.0 mile rollout to the launch pad.

Major elements of the SSV, consisting of the orbiter, solid rocket boosters (SRB) and external tank (ET) have required fatigue analyses as part of the mission life certification. Compared to rollout vibration, the SSV sees relatively high vibration loads during launch, ascent, descent and landing phases of the mission. Although preliminary measured SRB vibration levels during rollout were of low amplitude and frequency, the duration of the rollout phase is typically high, from 5-6 hours. As part of an expanded mission life assessment, additional certification effort was initiated to define fatigue load spectra for rollout.

This study addresses the CT vibration analyses in support of the rollout fatigue study. Structural models developed for modal and vibration analyses were used to identify unique CT, CT/MLP and CT/MLP/SRB vibration characteristics for comparison to instrumented rollout tests. Whereas the main structural and vibration characteristics of the SSV are well defined, minimum analytical and vibration test data on the Crawler Transporter were available. Unique vibration characteristics of the CT are attributable to the drive mechanism, hydraulic jacking system, structural framing and the CT-to-MLP support pad restraints. Initial tests performed on the CT/MLP/SRB configuration showed reasonable correlation with predicted mode shapes and frequencies.

INTRODUCTION

The Space Shuttle Vehicle (SSV), Figure 1, consisting of the orbiter, solid rocket boosters (SRB) and external tank (ET) undergoes periodic structural fatigue analyses as part of the mission life certification program. In addition to the high vibration occurring during the launch, ascent, descent and landing phases, additional fatigue analyses were required of the orbiter during rollout operations based on requirements for return-to-flight (RTF) certification for STS-114 Launch.

The SSV, assembled and mounted on the mobile launch platform (MLP) in the Vehicle Assembly Building (VAB), is lifted and transported to the launch pad by the Crawler Transporter (CT). Although vibration levels of the orbiter are low during rollout, durations can be 5-6 hours. As part of the RTF certification program instrumented tests were proposed for the CT/MLP/SRB, CT/MLP and CT rollout configurations to validate the analytical methods for predicting orbiter loads, load spectra and ultimately service life [1]. In conjunction with test data, existing finite element models of the SRB, MLP and recently developed CT model were used to predict mode shapes and frequencies for the various configurations. Prior to this effort no CT finite element model was available since initial structural certification was done in the 1960's.

SYSTEM OVERVIEW AND STRUCTURAL MODELS

Eight (8) interface holddown posts (HDP) support the SSV when mounted on the MLP – four (4) at each SRB aft skirt interface (See Figure 5). The HDP provides all the structural support between the SSV and the MLP during rollout, pre-launch and launch operations including quick release at lift off. The design of the MLPs provides integral stiffness to minimize flexure and loads to the SRB during all operational phases. The Space Shuttle Program (SSP) Integrated Vehicle and Loads Panel have done extensive structural modeling, development and certification for the SSV elements and MLP. These structural models, not covered in detail in this paper, are used for all aspects of system-to-system displacement, load, vibration and fatigue analyses.

1

Crawler Transporter Systems

The Crawler Transporter performs all lifting and transport operations of both the rollout of the MLP with the SSV and move operations of the MLP from the pad after launch (Figure 1). The CT provides vertical support for the MLP at four (4) pickup points. Lateral support is provided at three of the four points to minimize MLP-to-CT support constraint stresses (Figure 2). Jacking, equalization and leveling (JEL) of the MLP/SSV is performed by the JEL hydraulic system. Four hydraulic cylinders at each corner are pressurized by redundant pumps and provide for lifting and leveling control of the stack. Stack level is typically maintained to within ¼ inch with differential support loads at each corner set to within a prescribed tolerance. The CT drive system consists of four independently driven trucks each consisting of two tread belts driven by independent DC motors. DC generators run by diesel engines provide power to the four motors for each of the four trucks. (see Figure 3)

Crawler Transporter Structural Model

Figure 4 shows the typical structural subsystems modeled using the finite element analysis (FEA) code MSC/NASTRAN. These systems included the main chassis assembly, corner castings, truck framing and non-structural mass of all operational equipment. Mass properties and stiffness for these systems are very consistent and well defined based on 'as designed' or 'as built' configurations. However, three parameters that were not as definable and potentially of higher variability were 1) the JEL hydraulic system (vertical) stiffness, 2) the CT/MLP four-point pickup lateral constraints and 3) the crawlerway effective stiffness characteristics [2].

For the JEL system, dynamic response characteristics of the leveling system were considered sufficiently lower than system frequencies of concern and were not included in this analysis. Vertical stiffness was calculated based on hydraulic fluid bulk modulus properties (with allowance for entrained air) and piping system compliance. Lateral constraints, of the CT/MLP four-point pickup, have nonlinear frictional effects that were approximated by an equivalent spring based on the potential energy/stiffness principal. This was done based on the unknown frictional effects and the limitation of the linear analysis.

SRB and MLP Structural Models

SRB and MLP structural models were obtained from NASA's Loads Panel and were used for assessing the integrated response with the CT model (Figure 5). These combined models were used to determine overall effect of CT system characteristics on the response of the CT/MLP/SRB. Modifications to the existing MLP structural model included the addition of CT-to-MLP attached points, specific stiffness elements for the CT/MLP interface not previously incorporated in the MLP model and support points for the SRBs.

ROTATING EQUIPMENT AND MODAL ANALYSIS

Rotating Equipment Analysis

As part of identifying vibration sources within the CT/MLP/SRB systems, review and analysis was performed on all rotating equipment [3]. This was done, in part, to determine potential existing systems that would be main contributors to vibration and to identify extraneous frequencies that could be identified during testing. Systems that typically operated above 10 – 15 Hz, such as pumps, compressors, diesel engines and blowers, were above the range of concern. However, major systems such as the drive (propel) system were considered to be major contributors based on power and range of operational frequencies. Figure 6 shows the tread belt motors and gear train (two per tread belt) along with a gear reduction summary. As with all rotating equipment, vibrations typically occur at multiples of the primary operating RPM. For the gearing and track assembly, the low frequency shoe-to-ground pass mode was analyzed as a function of CT speeds from .3 to .9 MPH. These results are summarized in Table 1.

Modal Analysis

Modal analysis was performed on the three configurations used for tests. This included the CT/MLP/SRB, CT/MLP and the CT. For establishing the sensitivity of several parameters, cases were run to include the variation of the crawlerway stiffness, effective CT/MLP lateral support constraints and the JEL cylinder height. These parameters were run within their expected range as part of a parametric study.

ROLLOUT TESTS

Three instrumented configurations were planned for testing to provide data for identifying vibration characteristics, correlation to system models and establishing a basis for predicting actual vibration for the SSV STS-114 rollout planned for the spring of 2005. These tests included the CT/MLP/SRB, CT/MLP and CT configurations. At the time of this writing only the CT/MLP/SRB configuration was tested. This configuration (as shown in Figure 5) was instrumented with tri-axial accelerometers at the three levels of the MLP, at the lower part of the CT Trucks, at the CT/MLP interface (both on the CT and MLP side) and on the SRB stack located at several elevations. CT speed, wind conditions, JEL cylinder pressures and existing strain gage measurements on the SRB holdown posts were also part of the ensemble of instruments used to identify system characteristics. To identify vibrations unique to CT speeds, tests were run from .5 to .9 mph, with .9 mph being the typical maximum CT operational speed.

RESULTS AND COMPARISON

Sensitivity to crawlerway stiffness is apparent based on the modal analysis from the finite element models. Because crawlerway stiffness is difficult to measure an attempt to derive crawlerway stiffness from empirical data is presented. Along with this attempt to derive crawlerway stiffness for simulation efforts theoretical and measured results are presented for the first yaw mode of the CT/MLP/SRB configuration.

The hypothesis put forward regarding crawlerway stiffness is that a mode should be present characterized by rigid body motion of the crawler in the vertical 'x' direction. To test this hypothesis auto spectra were produced from accelerometers in locations 34, 35, 36 and 37. These locations are associated with the base of the JEL cylinders at crawler transporter corners A, B, C, and D respectively (see Figure 2 for reference locations). Along with the auto spectra, frequency response functions were generated using the Gyx/Gxx method with the accelerometer at location 34 used for the input auto spectrum. The amplitude and phase of the frequency response functions are used to identify modes that may be used to derive crawlerway stiffness. These modes will exhibit in-phase response for the accelerometers used in generating the frequency response functions. The amplitude and phase comparison results are presented in Table 2. The accelerometers at locations 34, 35, 36, and 37 are also used to identify the first 'yaw' mode of the CT/MLP/SRB configuration. To identify this mode the amplitude and phase in the 'y' direction at these locations is evaluated using the technique above to derive crawlerway stiffness. The results of this evaluation are presented in Table 3.

As part of the data correlation for rollout tests, modal analysis results were compared to frequencies from the CT/MLP tests at .9 MPH speed. This speed, which is approximate for this test, is held the longest during rollout to the PAD and would represent potentially the highest vibration conditions. Table 4 summarizes the predicted mode, primary direction and frequencies as compared to the modal test results. Modal test results were based on preliminary NASA Loads Panel process mode shapes and frequencies. However at the time of this writing, all frequencies and plots were not available.

General agreement between predicted and measured frequencies and mode shapes is very good. A distinction between natural and forced response vibration frequencies is made (under mode description) based on no predicted frequencies at .92, 1.77 and 2.71 HZ as compared to measured results. The fundamental drive frequency, as referenced in Table 1 related to shoe pass, correlates well with measured. The higher drive frequencies, which are multiples of 2 and 3 of the fundamental drive frequency, are believed to be due to the tread belt mechanism and/or interaction of the independent corner trucks. This same phenomenon was observed at .7 MPH where drive frequencies exhibited the same 1, 2 and 3 multiples of drive speed.

CONCLUSIONS

Frequency response analysis of accelerometer data from locations 34, 35, 36, and 37 did not identify a modal response associated with crawlerway stiffness. Nor did the analysis identify the first system yaw mode. Possible reasons for the inability to identify these modes are 1) the Gyx/Gxx frequency response method is susceptible to noise on the input channel used for calculating the input auto spectra, Gxx, 2) the auto spectra have dominant responses at multiples of the shoe pass frequency masking the low amplitude responses associated with ground stiffness. Further signal processing is required to derive a method to account for these phenomena. In conjunction with additional processing of the 0.9 mph data similar signal processing of data from alternate speed tests is recommended. Processing of data from alternate speed tests and subsequent correlation tests will assist in identifying natural modes of the CT/MLP system. For predicting natural system frequencies, this method seems

fairly good. However, additional tests that have been delayed for the CT/MLP and CT is needed for defining sources of drive mechanism frequencies and for correlating unique characteristics for each configuration.

ACKNOWLEDGEMENT

REFERENCES

1. Integrated Test Requirements for Rollout Fatigue Loads Spectra Methodology Verification, NASA NSTS 60512, (October, 2003)

2. Deese, J.H. and Whisenant, C.C., "Crawlerway Feasibility from Design Analysis", Advanced Studies Office, NASA (September, 1963)

3. "Crawler Transporter (CT) & Min-Portable Purge Unit (MPPU) Rotating Equipment Summary – in Support of Rollout Fatigue Spectra Analysis Study", NASA/United Space Alliance Briefing to NASA Loads Panel, (November, 2003)

4. "Crawler Transporter (CT)/MLP System Overview/Structural Models – in Support of Rollout Fatigue Spectra Analysis", NASA/United Space Alliance Briefing to NASA Loads Panel (November, 2003)
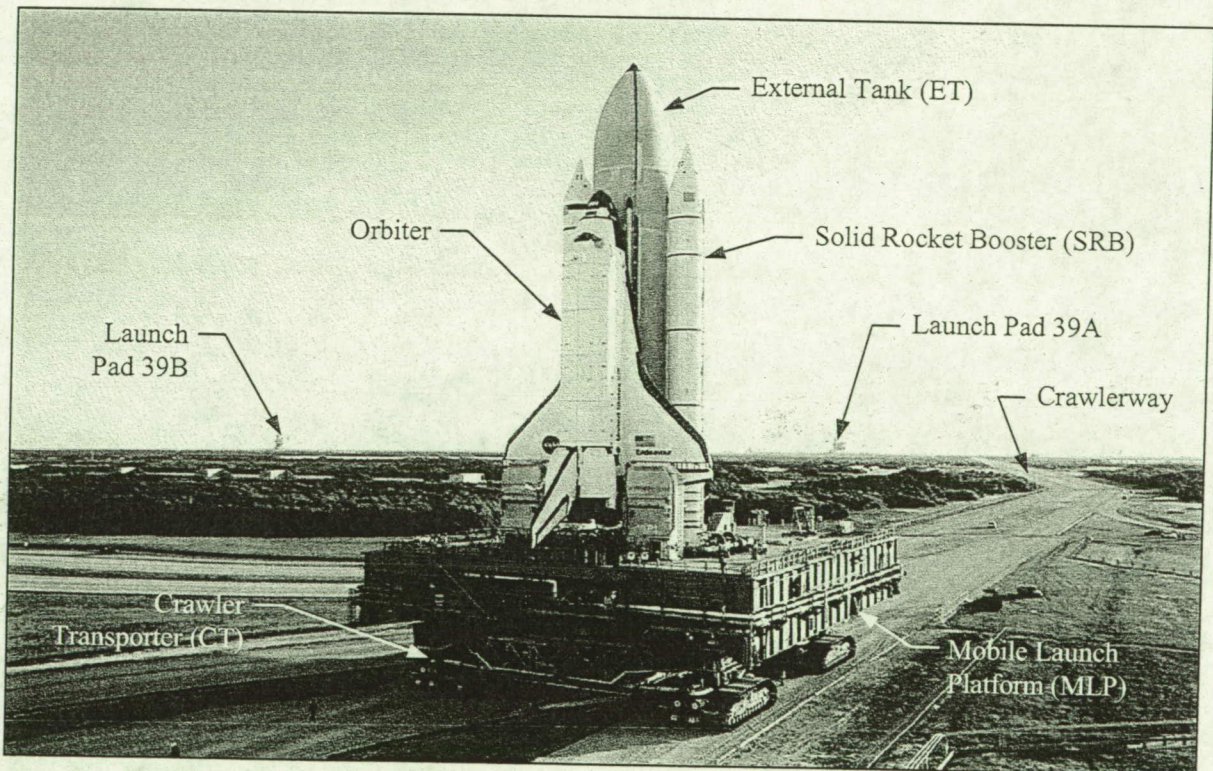
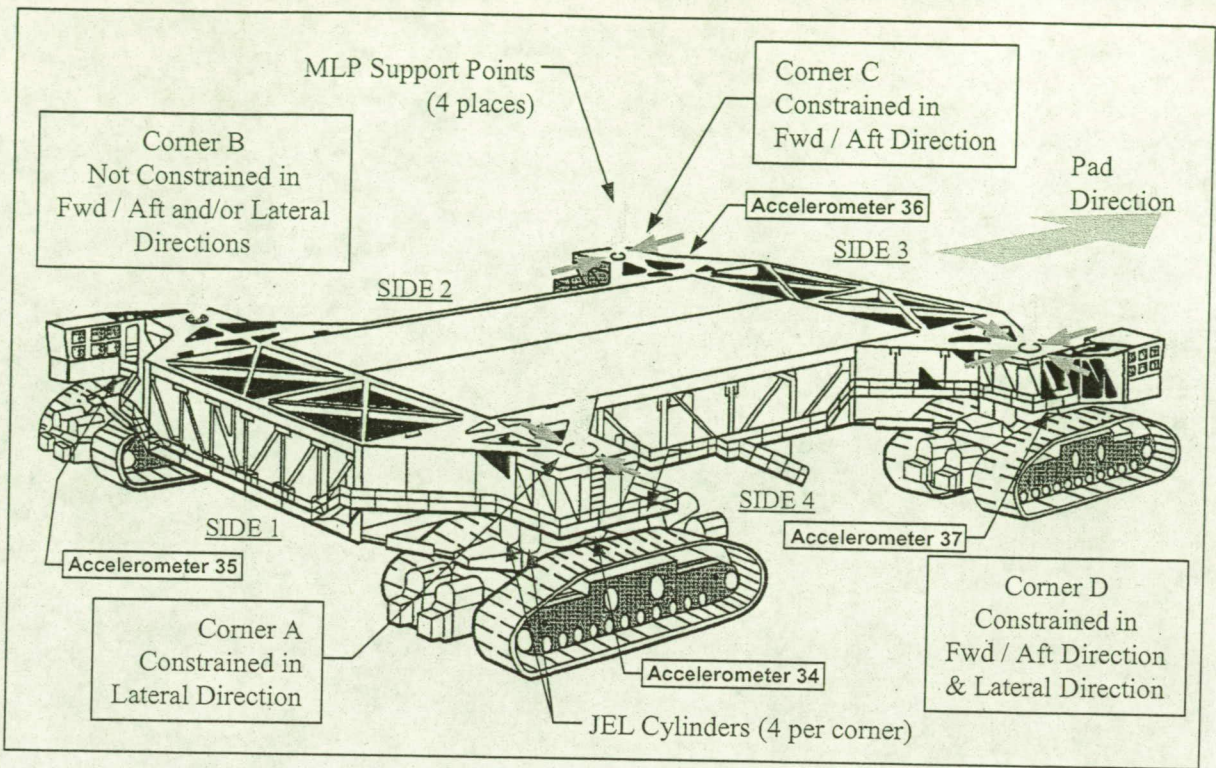*Figure 1. CT, MLP, and SSV Rollout to Launch Pad*

Figure 2. Crawler Transporter (CT) Main Support System

MLP Support Points (4 places)

Corner B Not Constrained in Fwd / Aft and/or Lateral Directions

Corner C Constrained in Fwd / Aft Direction

Accelerometer 36

Pad Direction

SIDE 2

SIDE 3

SIDE 4

SIDE 1

Accelerometer 35

Accelerometer 37

Corner A Constrained in Lateral Direction

Accelerometer 34

Corner D Constrained in Fwd / Aft Direction & Lateral Direction

JEL Cylinders (4 per corner)
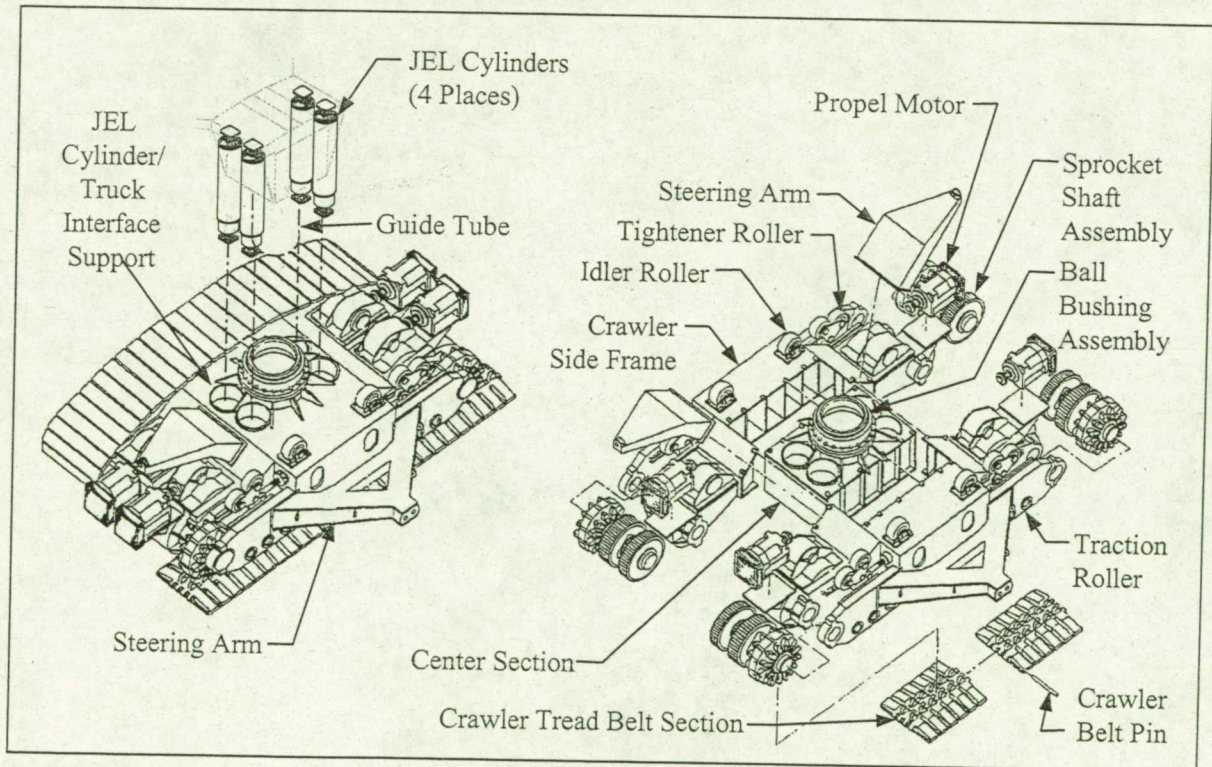
Figure 3. Crawler Transporter (CT) JEL System, Truck Assembly and Drive (Propel) System

JEL Cylinders (4 Places)

JEL Cylinder/ Truck Interface Support

Guide Tube

Propel Motor

Steering Arm

Tightener Roller

Idler Roller

Crawler Side Frame

Sprocket Shaft Assembly

Ball Bushing Assembly

Steering Arm

Center Section

Crawler Tread Belt Section

Traction Roller

Crawler Belt Pin

Figure 4. Crawler Transporter Structural Model

Figure 5. SRB, MLP, and CT Structural Model

Figure 6. Crawler Transporter (CT) Drive (Propel) System Gearing and Tread Belt Drive Sprocket

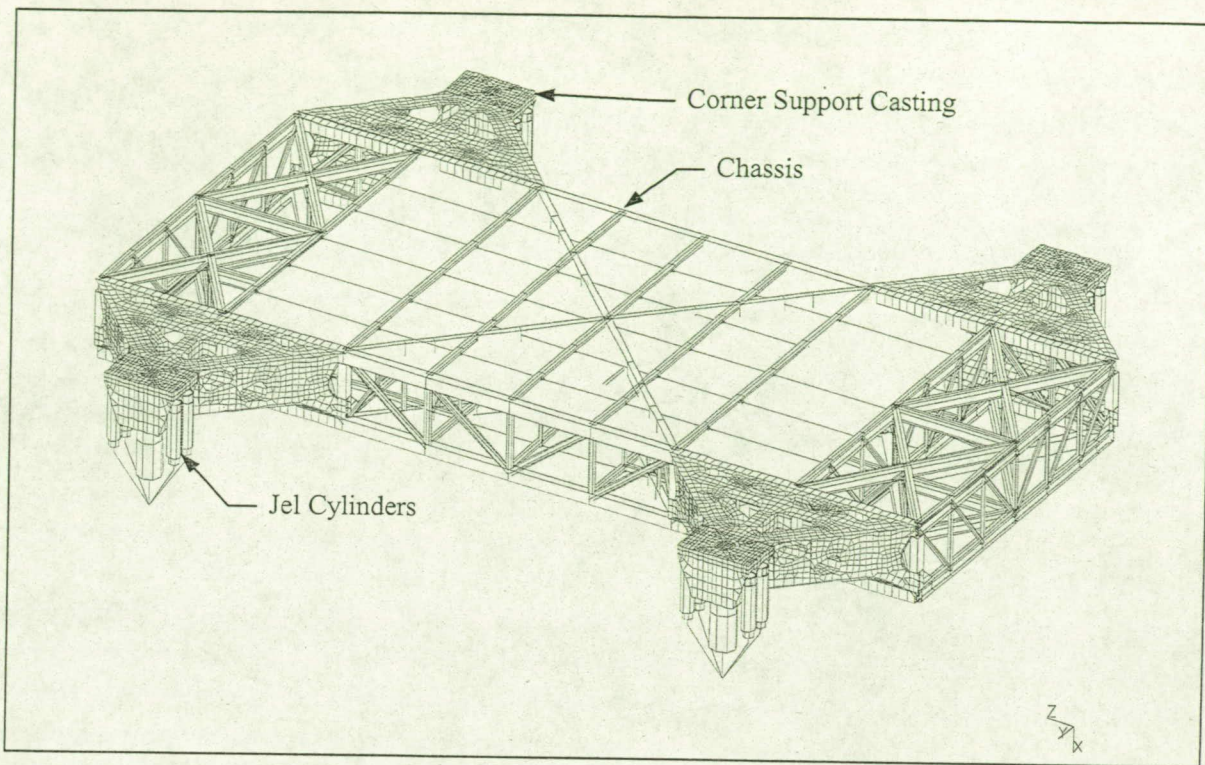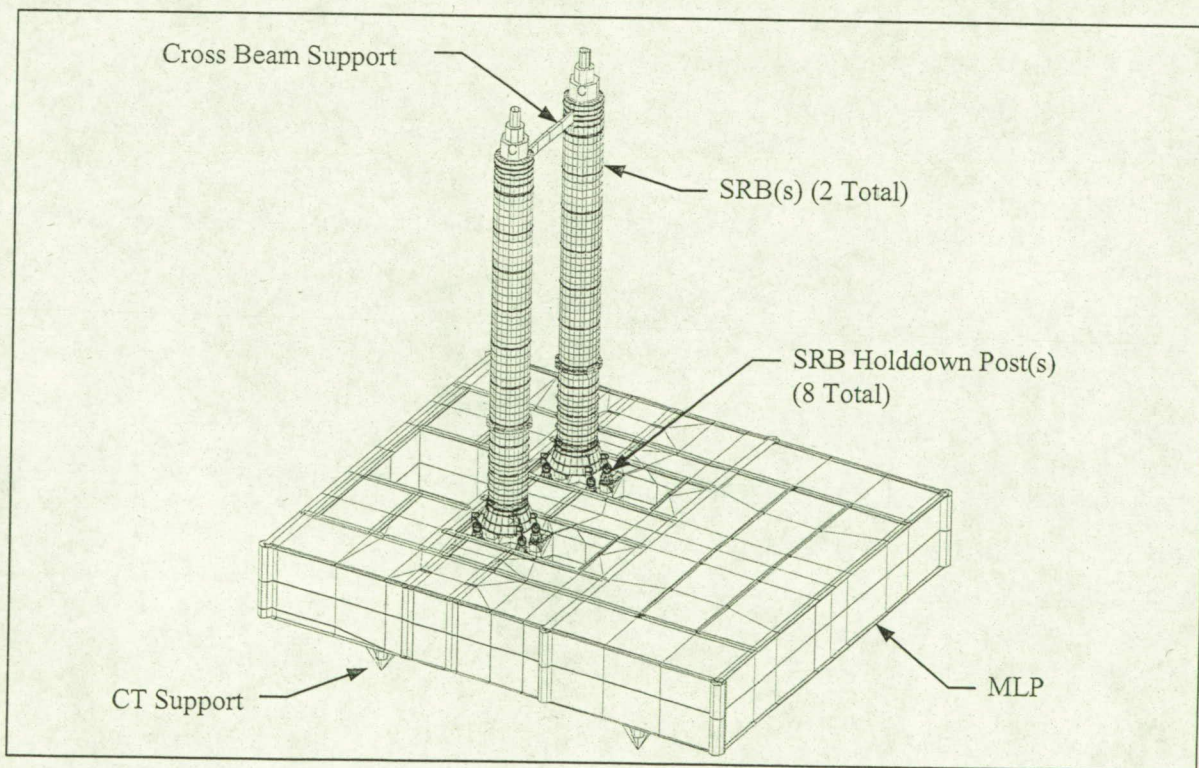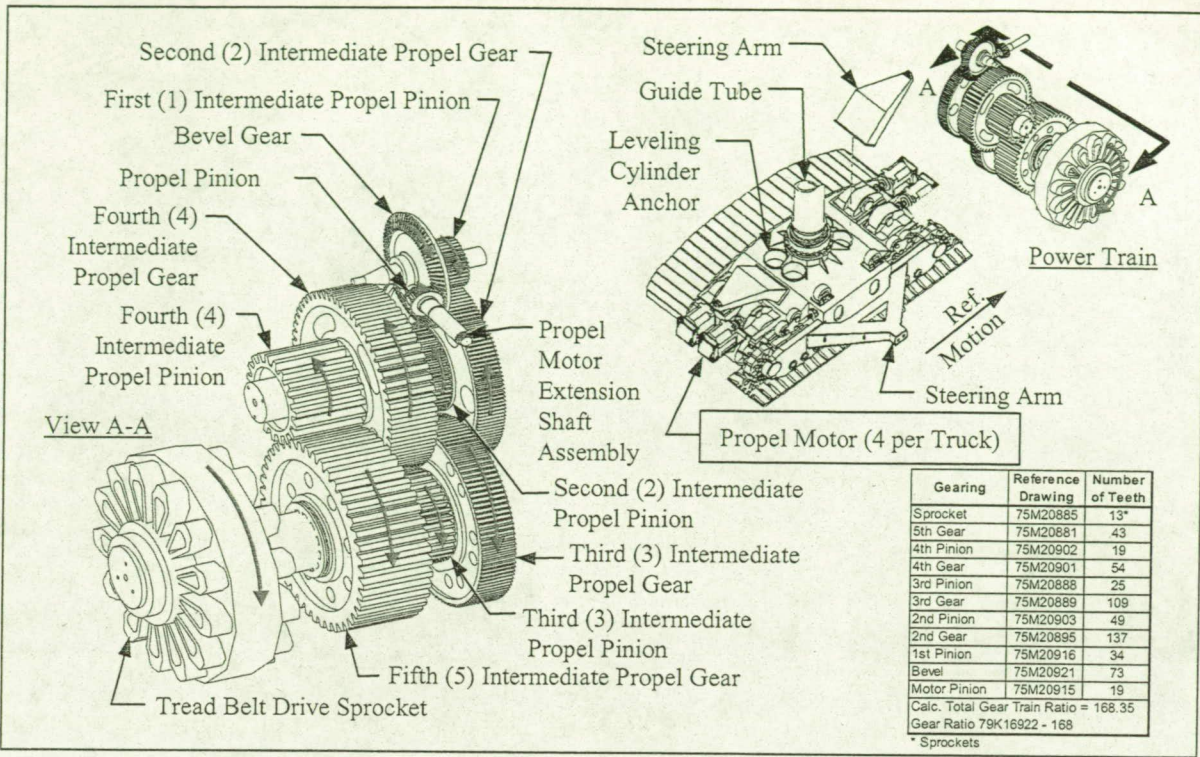*Table 1. Propel Motor, Gearing, and Shoe Pass at Various CT Speeds*

CT Speed (MPH) =>	0.9	0.8	0.7	0.6	0.5	0.4	0.3
Impact Sources (in order of rate)	Cycles or impacts per second						
Sprocket / 5th Shaft Rotation	0.068	0.060	0.053	0.045	0.038	0.030	0.023
4th shaft	0.15	0.14	0.12	0.10	0.08	0.07	0.05
3rd shaft	0.33	0.29	0.26	0.22	0.18	0.15	0.11
2nd shaft	0.73	0.65	0.57	0.49	0.41	0.33	0.24
Shoe Pass	**0.88**	**0.78**	**0.68**	**0.54**	**0.49**	**0.39**	**0.29**
4th / 5th tooth impact	2.90	2.58	2.26	1.94	1.61	1.29	0.97
1st shaft rotation	2.96	2.63	2.30	1.97	1.64	1.32	0.99
3rd / 4th tooth impact	8.26	7.34	6.42	5.50	4.59	3.67	2.75
Motor shaft	11/37	10.11	8.85	7.58	6.32	5.05	3.79
2nd / 3rd tooth impact	36.00	32.00	28.00	24.00	20.00	16.00	12.00
1st / 2nd tooth impact	100.64	89.46	78.27	67.09	55.91	44.73	33.35
Bevel / Pinion tooth impact	216.08	192.07	168.06	144.05	120.04	96.03	72.03

7

Table 2. Phase Comparison for Four Corners of Crawler Transporter

Frequency	FRF(34) X-sense Amplitude and Phase (degrees)							
	34		35		36		37	
	Amp.	φ	Amp.	φ	Amp.	φ	Amp.	φ
3.625	-	-	0.07	-71.3	0.21	-63.2	.11	-70.6
5.201	-	-	0.04	-165.9	0.030	-157.9	0.05	-156.1
5.726	-	-	0.01	-161.9	0.04	-162.1	0.08	-157.1
5.951	-	-	0.05	-176.6	0.02	-181.2	0.10	-174.7

Table 3. Phase Evaluation of Four Corners of Crawler Transporter

Frequency	FRF(34) Y-sense Amplitude and Phase (degrees)							
	34		35		36		37	
	Amp.	φ	Amp.	φ	Amp.	φ	Amp.	φ
0.550	-	-	1.62	-13.6	1.61	-21.7	1.81	-18.0
1.025	-	-	3.26	-345	3.59	-347.4	1.62	-335
1.25	-	-	3.60	-15.5	3.66	-6.9	1.29	-6.5
2.675	-	-	1.04	-220.0	0.68	-218	0.14	-193
4.45	-	-	0.57	-16.3	0.35	-36.9	0.93	-60.1

Table 4. CT/MLP Modal Test Results ~ 0.9 MPH

Nastran Analysis Results				Modal Test Results	
Mode Description	Direction*	Mode No.	Freq. (Hertz)	Disp. Set No.	Freq. (Hertz)
Bending Mode of SRB's	RZ	1	0.43	1	0.46
Bending Mode of SRB's	RY	2	0.58	2	0.58
Bending Mode of SRB's	RY	3	0.78	3	0.67
Forced Vibration	Z	N/A	N/A	4	0.92
Forced Vibration	RX	N/A	N/A	5	1.77
System Longitudinal Mode	Z	4	2.09	6	2.02
Bending Mode of SRB's	RZ	5	2.10	7	2.18
System Lateral Mode	Y	6	2.36	N/P	N/P
System Yaw Mode	RX	7	2.57	8	2.44
Forced Vibration	Z	N/A	N/A	9	2.71
System Vertical Mode	X	10	3.36	10	3.40
Bending Mode of SRB's	RZ	11	3.47	N/P	N/P
System Pitch Mode	RY	12	3.65	N/P	N/P
Bending Mode of SRB's	RY	13	3.70	11	3.61
Bending Mode of SRB's	RY	14	3.86	12	3.80
System Roll Mode	RZ	15	4.50	13	4.37
CT/MLP Bending Mode	RY, RZ	21	5.29	14	5.33
CT Bending Mode	RY	22	5.51	15	5.51
Torsion Mode of SRB's	RX	23	5.77	N/P	N/P
Torsion Mode of SRB's	RX	24	5.93	N/P	N/P
Bending Mode of SRB's	RZ	25	6.05	N/P	N/P
CT/MLP Bending Mode	RY,RZ	26	6.19	N/P	N/P
Torsion (Twist) Mode of CT/MLP	RY, RZ	31	6.41	16	6.29

* RX, RY & RZ - Rotation about X, Y & Z , respectively   N/P - No Plot, N/A- Not Available